physchem

MDPI

Review

Molecular Terms of Dioxygen and Nitric Oxide

Igor V. Khudyakov [1,*] and Boris F. Minaev [2]

[1] Department of Chemistry, Columbia University, New York, NY 10027, USA
[2] Department of Chemistry and Nanomaterials Science, Bohdan Khmelnytsky National University, 18031 Cherkasy, Ukraine; bfmin43@ukr.net
* Correspondence: startatj@aol.com

Abstract: Molecular terms of dioxygen and nitic oxide are presented. Electron spin resonance spectra of diatomic molecules corresponding to these terms are discussed. Gas-phase ESR can be a convenient method of monitoring paramagnetic pollutants in the atmosphere. We ran additional calculations in molecular physics for terms of these molecules and Zeeman transitions.

Keywords: ESR; pollutants; gas phase; terms of diatomic molecules; electronic structure of diatomic molecules; ESR spectra of singlet dioxygen; nitric oxide

Citation: Khudyakov, I.V.; Minaev, B.F. Molecular Terms of Dioxygen and Nitric Oxide. *Physchem* **2021**, *1*, 121–132. https://doi.org/10.3390/physchem1020008

Academic Editor: Jacinto Sá

Received: 11 May 2021
Accepted: 17 June 2021
Published: 1 July 2021

1. Introduction

Pollution of the atmosphere is becoming a more and more important problem for humanity every year [1]. It is important to monitor the concentration of pollutants from the standpoint of the safety of a population. Some of the pollutants are paramagnetic and demonstrate electron spin resonance ESR spectra in the gas phase. In this mini-review, we consider the electronic structure and magnetic properties of two pollutants: singlet dioxygen ($^1O_2$) and nitric oxide (^2NO) in the gas and the liquid phase as well as their ESR spectra. It is demonstrated that an X-band ESR is a promising tool for detecting and monitoring these two pollutants.

2. Electronic Terms of Dioxygen and Nitric Oxide

The molecular term symbol of the ground and some excited state of these diatomic radicals are determined in a short presentation by the total electronic spin angular momentum (S), by its projection S_z on the molecular *z*-axis (Σ) [2], by the orbital angular momentum z- projection (Λ), as well as their sum—total electronic momentum projection $\Omega = S_z + \Lambda$ [2–4]. The quantum numbers for the observed values of projections of these momenta on the internuclear axis of a diatomic molecule are denoted as Σ, Ω, and Λ, and $\Omega = |\Lambda + \Sigma|$. According to a common convention [2–6], the states with Λ = 0, 1, 2, are denoted by Σ, Π, Δ symbols. (One should distinguish notations of spin projection and the case of Λ = 0, which are denoted by the same symbol Σ).

The quantum numbers, which determine the measured absolute value of the total spin and its projection on the *z*-axis, are fixed in the quantum theory of angular momentum as eigenvalues of the corresponding square S^2 operator and the S_z operator [5]:

$$\vec{S}^2\Psi = S(S+1)h^2\Psi; \qquad S_z\Psi = \Sigma h\Psi \tag{1}$$

where *h*-bar is $h = h/2\pi$ as usual and *h* is the Planck constant.

For the singlet $^1O_2$ ($^1\Delta_g$) and triplet $^3O_2$ ($^3\Sigma_g{}^-$) state dioxygen, the spin quantum number is equal to S = 0 and S = 1, respectively. In the last case, the spin projection quantum number has values Σ = 0, ±1. For the zero S singlet state the projection is naturally absent (Σ = 0). In the case of the ground state ^2NO radical S = 1/2, Σ = ±1/2 and two Ω values are possible (3/2 and $\frac{1}{2}$). For analysis of ESR and optical spectra of diatomic molecules,

one has to consider rotational nuclear angular momentum R [2–4]. R is an operator related to the rotation of nuclei as a whole. Because of the axial symmetry of the field in diatomic molecules, only the orbital angular momentum projection of electrons on the *z*-axis can be observed as a constant of motion [2]. For the π^2 open shell of dioxygen, there are two possibilities for the electronic wave functions Ψ of states with $\Lambda = 0$; function Ψ can either change sign upon reflection in any plane, which contains internuclear axis z (Σ^- state), or not change sign (Σ^+ state). These symmetry restrictions are connected with a general property of all electrons in respect to their permutation [4,5]. For the triplet state ($^3\Sigma^-$), the spin part of the wave function is symmetric, but the spatial part is asymmetric in respect to permutation; this leads to a sign change upon reflection in a molecular plane since π^+ transforms to π^- [4].

Terms may include one or two additional notions related to operations of symmetry of a molecule, namely g/u for homonuclear diatomic species, like O_2, with the inversion symmetry center or $+/-$ in case $\Lambda = 0$. We will present the terms including these notations like it is presented in the literature [2–6]. The total angular momentum is denoted as $J = \Lambda + R + S$. The two additional notations are unimportant in the context of this mini-review. The contribution of nuclear momentum I and rotational momentum R into *J* are mostly omitted here since main isotope ^{16}O has no nuclear spin and for the $^1O_2$ ($^1\Delta_g$) molecule, we will consider the ESR spectrum for the lowest rotational state R = 0. Detailed information on the terms of diatomic molecules can be found in ref. [2–6].

The terms are presented as $^{2S+1}\Lambda_\Omega$. Spin S of one electron is $\frac{1}{2}$ and $M_s = \pm\frac{1}{2}$. Here, M_S is a spin component along the field. The total spin quantum number S is used in the superscript of a term to denote the term multiplicity m = 2S + 1. Thus $^1\Lambda_\Omega$, $^2\Lambda_\Omega$, and $^3\Lambda_\Omega$ correspond to a singlet state, doublet state (a radical), and a triplet state of a diatomic molecule, respectively. We deal with two molecules that have the highest occupied $2\pi^*$ molecular orbital–antibonding π orbitals. The individual electron on two degenerate π^*—orbitals has a projection of orbital momentum as quantum number $\lambda = \pm 1$. When we deal with two degenerateπ- orbitals, it is necessary to ascribe $\lambda_1 = +1$ to an electron on one orbital and $\lambda_2 = -1$ to another. Projection of a total orbital momentum for two electrons in the open $2\pi^*$ shell $\Lambda = \lambda_1 + \lambda_2$ is denoted Σ, Π, and Δ for $\Lambda = 0$, 1, and 2, respectively.

ESR studies of dioxygen and nitrous oxide have been performed by numerous researchers [7–18], but for their practical application in analytical purposes, we need to generalize common physical backgrounds and clarify some details that have not been considered yet.

The terms of heteronuclear diatomic radicals, $^2\Pi_\Omega$ (like the ground state of ^2NO molecule) has the index $\Omega = \Lambda + S_z$. Typical values of Ω are $\frac{1}{2}$, 3/2. Transitions between different states in ESR spectra are allowed at $\Delta M_J = \pm 1$. Here, M_J is a quantum number of the component of J, which is a total angular momentum, see above. $M_J = \pm 1/2, \pm 3/2$. We simplify the situation by ignoring molecular rotation in this case, which is acceptable for our goal.

Scheme 1 below presents an occupation of the highest molecular orbitals by electrons in these two species:

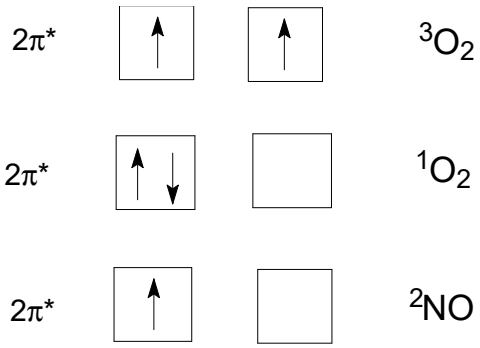

Scheme 1. The highest occupied molecular orbitals (MO) of the two species.

Table 1 below presents terms of diatomic molecules of interest and existence or a lack of corresponding EPR spectra in the gas and in the liquid phase. It is instructive to compare EPR data on the same species in the gas and in the liquid phase, see Table 1.

We discuss the individual terms of Table 1 below.

Table 1. The terms of O_2 and ^{2}NO in the ground and the closest in energy excited states as well as their paramagnetism in the gas and the liquid phases.

Molecule	Ground State Term	ESR [1] in the Following State	Term of the Nearest Excited State	ESR [1] in the Following State
O_2	$^3\Sigma_g^-$	Liquid: **No** [2] Gas: **Yes**	$^1\Delta g$	Liquid: **No** Gas: **Yes**
NO	$^2\Pi_{1/2}$	Liquid: **No** [3] Gas: **No**	$^2\Pi_{3/2}$	Liquid: **No** Gas: **Yes**

[1] X-band spectrometer. [2] See the text below. [3] Electronically-excited state.

3. Dioxygen

Molecular oxygen (dioxygen) possesses a ground triplet state $^3O_2$ ($^3\Sigma_g^-$). Triplet oxygen $^3O_2$ demonstrates a very broad (width of ca. 1 T [7]) weak ESR spectrum in the liquid phase at low temperatures. Orbital angular momentum has a large contribution to the magnetism of molecules and in the case $^3O_2$ ($^3\Sigma_g^-$) $\Lambda = 0$. Additionally, molecular rotations are quenched by the solvent. ESR of $^3O_2$ is not observed in liquid solutions at room temperature.

Molecules in the gas phase undergo free rotation. At the same time, they have quantized energy levels [2]. Rotation of a molecule leads to the appearance of local magnetic fields, and these fields interact with an electronic spin magnetic moment in triplet state $^3O_2$ ($^3\Sigma_g^-$) and with orbital magnetism in the excited singlet $^1O_2$ ($^1\Delta g$) oxygen. The rotation levels make an infinite ladder of spin-energy levels and rotational levels are inseparably interlaced with magnetic levels [2]. This way, the ESR spectrum of $^3O_2$ consists of a huge number of components (lines). An intensive ESR spectrum is observed in the gas phase under low pressure, see Figure 1:

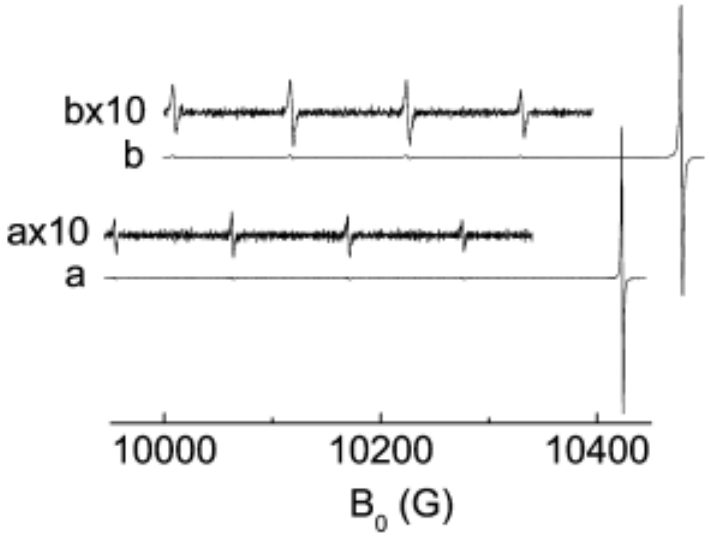

Figure 1. The ESR spectra in the sealed cell containing $^3O_2$ (P_{O2} = 0.2 Torr) and a sensitized naphthalene vapor obtained in the dark (**a**) and during irradiation of a sensitizer (**b**), T = 293 K. The intensity component in the high field (**a**,**b**) is part of the ESR of $^3O_2$ ($^3\Sigma_g^-$). The ESR spectrum of $^1O_2$ ($^1\Delta g$) consisting of four components (b and b × 10, a and a × 10) was obtained under photoexcitation of naphthalene in the presence of $^3O_2$. Adapted from ref. [9].

The nearest in energy to the ground triple $3O_2$ ($^3\Sigma_g^-$) dioxygen is the electronically-excited state $^1O_2$ ($a^1\Delta g$); it provides another ESR spectrum (see Scheme 1 and Table 1). Singlet dioxygen ($^1\Delta g$) is 94 kJ/mol above the triplet ground state. There are many ways to generate labile singlet dioxygen [9,10,12–14,17,19]. Singlet O_2 ($^1\Delta g$) molecule does not have spin (S = 0) but has an electronic orbital angular momentum $\Lambda = 2$ [9–17]. Together with the rotational angular momentum (R), they form a total angular momentum, $J = \Lambda + R$; it is quantized along the magnetic field axis with quantum number M_J. The O_2 ($^1\Delta g$) molecule belongs to the classical Hund's case (a) when Λ is quantized along the molecular z-axis [2]. Values Λ and J in this case are good quantum numbers [3]. Thus, for the free rotating O_2 ($^1\Delta g$) molecule in the gas phase, the total momentum J provides an ESR spectrum [9,13]. The Λ-doubling in the O_2 ($^1\Delta g$) molecule is expected to be very small [4,18], in fact, neither we nor other authors [19] could resolve the Λ—doubling splitting in the singlet oxygen ESR spectrum. Zeeman energy of O_2 ($^1\Delta g$) in an external magnetic field H can be described by the following equation for magnetic field interaction with molecular magnetic moment [13,20]:

$$E_J = \mu_B g_L H M_J \frac{(\Lambda + 2\Sigma)(\Lambda + \Sigma)}{J(J+1)} = \mu_B H M_J g_J \quad (2)$$

The spin angular momentum projection is absent ($\Sigma = 0$) for the singlet oxygen and we have relation: $g_J = g_L \Lambda^2 / J(J+1)$. For the lowest rotational level ($J = \Lambda = 2$) we have $g_J = 2\, g_L/3$ [13]. The electronic magnetic moment along molecular axis z is equal to $2\, g_L \mu_B$, where $\mu_B = eh/2mc$ is the Bohr magneton and g_L is the electronic orbital angular momentum g-factor, which is close to unity [13]; small corrections to g-factor of the singlet O_2 ($^1\Delta g$) state are important for the EPR spectrum and are considered below.

Since $g_L \approx 1.0$ and $g_J \approx 2/3 \approx 0.667$, all allowed transitions with $\Delta M_J = \pm 1$ in the ESR spectrum of $^1O_2$ ($^1\Delta g$) dioxygen should have the same transition energy of about $\frac{2}{3}\mu_B H$. Only one transition $0 \rightarrow 1$ is close to the $0.667\ \mu_B H$ resonance [20], but all others are shifted [9].

In the absence of electron-rotational interaction, all four EPR transitions in the ground state ($J = \Lambda = 2$) of the singlet ($^1\Delta g$) dioxygen would be observed at the same field about $H \approx 10$ kG with the frequency (9624.92 MHz) of X-band ESR spectrum. Transition energies $h\nu_i$ in the EPR spectrum (Figure 1) are different (at a fixed field H) because of perturbations from the upper rotational $J = 3$ levels (see Figure 2 below). They are equal to 0.65597 for $(-2 \rightarrow -1)$ transition, 0.66264 $(-1 \rightarrow 0)$, 0.66954 $(0 \rightarrow +1)$ and 0.67667 $(+1 \rightarrow +2)$ in the units $\mu_B H$ [9,13], see Table 2 below. Thus, we have almost symmetrically split quartet EPR lines (Figure 1). At the fixed microwave frequency $\nu = 9.62492$ GHz, the ESR X-band resonance signals are obtained at the magnetic field strength of about 10 kG, respectively [9]. The account of interaction with the first excited rotational level R = 1($J = 3$) provides additional corrections to M_J sublevels of the ground rotational state $J = 2$ in the second-order of perturbation theory; the results are presented in Figure 2 below [13].

One can see from Table 2 and Figure 2 that the splitting between nearest transition is equal to $2a$, which depends on the ratio of magnetic field H^2 and equilibrium rotational constant B_e of $^1O_2$ ($^1\Delta_g$). Here $a = (2\mu_B H)^2 / 378 B_e$.

Table 2. Second-order corrections for $J = 2$ $^1O_2$ ($^1\Delta g$) spectrum of the X band ESR signals.

ESR Transition	Field (G)	$h\nu_i/\mu_B H$ [1]	$h\nu_i/\mu_B H$ [2]	Second-Order Correction [2]
$(-2 \rightarrow 1)$	10,486.00	0.655	0.65597	$\nu_0 + (5-8)a$
$(-1 \rightarrow 0)$	10,375.68	0.662	0.66264	$\nu_0 + (8-9)a$
$(0 \rightarrow +1)$	10,264.67	0.669	0.66954	$\nu_0 + (9-8)a$
$(+1 \rightarrow +2)$	10,151.75	0.677	0.67667	$\nu_0 + (8-5)a$

[1] Observed [9]. [2] Calculated by second-order correction [12,20].

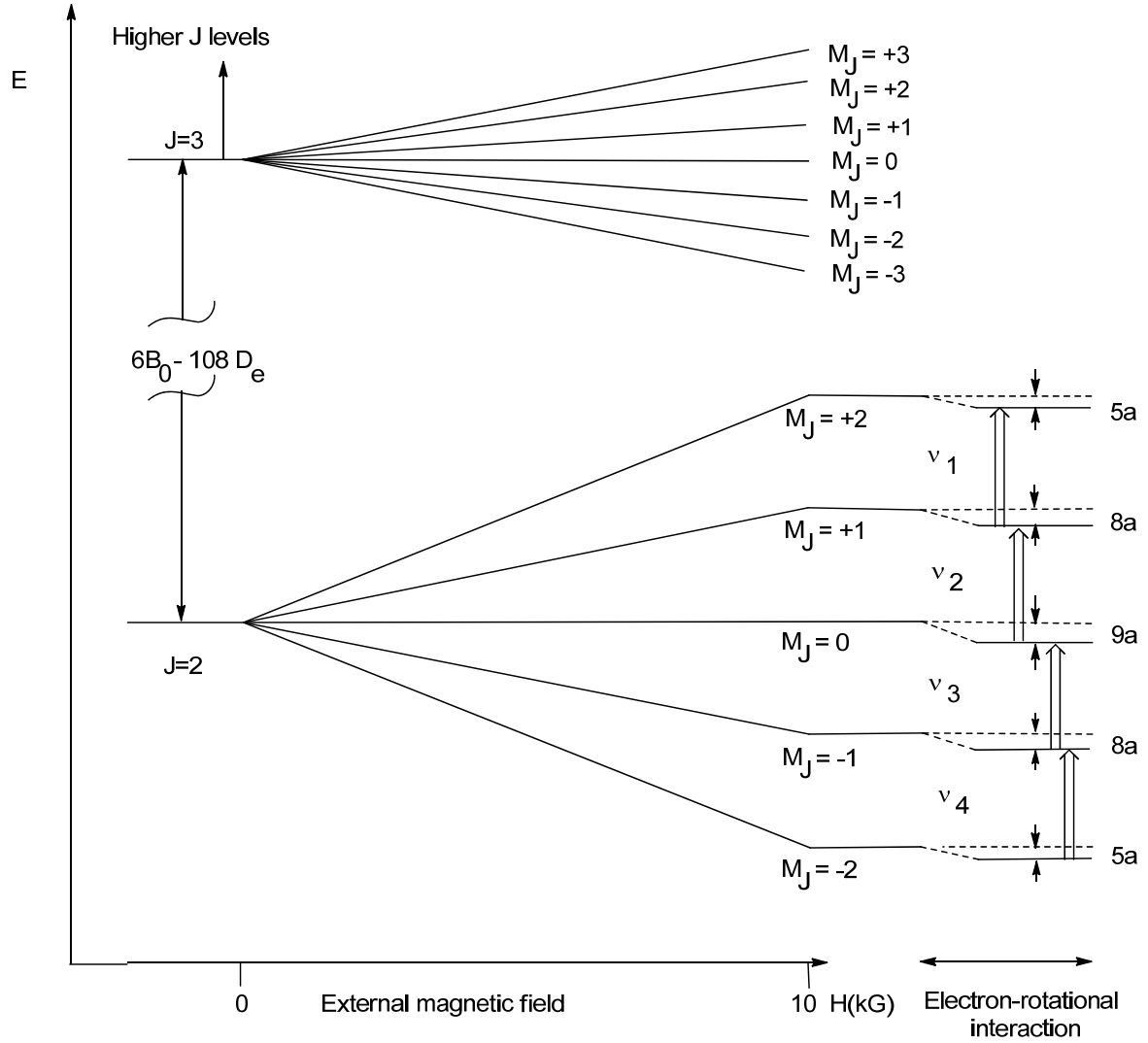

Figure 2. Splitting of the ground and first excited rotational levels of the singlet oxygen $^1O_2$ ($^1\Delta_g$) state in magnetic field *H*. Generalized from refs. [13,20]. Here D_e is centrifugal distortion parameter, B_o is the rotational constant in the lowest vibrational level; see for details ref. [20].

This prediction agrees well with the observed quartet splitting in ESR spectra of singlet dioxygen in the gas phase [9,13,20].

There is no EPR spectrum of $^1O_2$ ($^1\Delta_g$) in the liquid phase since the local electric fields of solvent molecules quench the orbital angular momentum [2]. At any oxygen collision with a solvent molecule, the local electric fields remove the degeneracy of the ($^1\Delta_g$) state; it splits into two close-lying sublevels which position depends on the particular geometry of any new collision and orbital angular momentum Λ is not anymore a good quantum number. (Non-zero orbital angular momentum can exist only in degenerate states) [21]. Thus, the simple Zeeman energy picture, Equation (1), is completely distorted and rotational coherence is quenched.

High accuracy of ESR measurement in the gas phase provides a good agreement between perturbation theory and the observed quartet splitting in the ground rotational level $J = 2$ of singlet oxygen [13,20]. However, this accuracy leads to additional problems with exact values of g_L-factor.

Rotational g_L-factor contains small contributions from relativistic mass-velocity dependence [20] and non-diagonal orbital momenta terms responsible for mixing of different states induced by the shift operator L_+ and L_-. Similar contributions in combination with spin-orbit coupling (SOC) perturbation are responsible for the anisotropy of electronic spin

g-factor; they are rather important for the ground triplet state of dioxygen $^3O_2$ ($^3\Sigma_g^-$) and provide ESR signal deviation from the free-electron value (g_e = 2.0023). This deviation is big for the perpendicular component of g-tensor (as much as $g_\perp$ = 2.0052 [3,22]), while $g^{||}$ is close to g_e value [23,24]. These parameters were first obtained fro314 m the ESR spectrum of solid oxygen [3] and these parameters are supported by ab initio self-consistent field (SCF) calculations [22,24]. The electronic spin g-factor is connected with the spin-rotational coupling constant (γ) approximation is well developed for the ground and excited triplet states $^3\Sigma^-$ of dioxygen [24]. However, for the singlet O_2 ($^1\Delta_g$) molecule, the rotational g-factor theory contains some discrepancies which will be shortly discussed [13,20].

4. A Short Introduction to the Theory of Rotational g-Factor for the Singlet O_2 ($^1\Delta_g$) Molecule

The rotational g_L-factor includes the nuclear part g_r^N and the orbital part g_r^e [25]. The nuclear rotational g-factor is simply determined by atomic mass (M_A) and charge (Z_A); it corresponds to the moment for bare nuclei of two atoms A and B [4]. It does not contribute to the energy of the lowest rotational level K = 0 of the O_2 ($^1\Delta_g$) molecule.

$$g_r^N = m_p \frac{Z_A M_B^2 + Z_B M_A^2}{(M_A + M_B) M_A M_B} = 2.723 \times 10^{-4} \quad (3)$$

The orbital part in the first order of perturbation theory is equal [25]:

$$g_r^e = \frac{2m_p}{m_e \mu R^2} \sum_{n \neq 0} \frac{|\langle \Psi_0 | \sum_i l_{i,\perp} | \Psi_n \rangle|^2}{E_0 - E_n} \quad (4)$$

where m_p, m_e, μ are a mass of proton, electron and reduced mass of dioxygen, R is the internuclear distance, $l_{i,\perp}$ is the perpendicular component of the orbital angular momentum operator for the i-th electron, Ψ_n, E_n are eigenfunction and energy of the n-th singlet state of O_2 [24–26]. The main contributions to the sum (4) provide $^1\Pi_g$, $^1\Phi_g$ states [24]. The lowest $^1\Pi_g$ state produces the largest contribution (-3.143×10^{-4}) at the equilibrium R_e distance [25]. Complete active space (CAS) linear response calculations [24] predict a value of -3.896×10^{-4}, which is in good agreement with the experimental estimation of $(-3.957 \pm 0.025) \times 10^{-4}$ obtained in ref. [20].

The electronic rotational ${g_r}^e$-factor represents the magnetic moment produced by the rotation of "electrons following the nuclei" during molecular rotation [13]. Miller [20] has compared this electronic rotational ${g_r}^e$-factor for the $^1O_2$ ($^1\Delta_g$) state with ${g_r}^e$-value for the ground $3O_2$ ($^3\Sigma_g^-$) states [$(-3.98 \pm 0.12) \times 10^{-4}$], also extracted from the experiment [3], and noted that they coincide within the experimental error.

Arrington et al. [13] have obtained S-band EPR spectra at 3 GHz for J = 2 and J = 3 levels (only two of six transitions for J = 3 spectrum were detected because of high field resonances). The $g_J = 4g_L/J(J+1)$ values obtained from the S-band spectra are consistent within the H field measurement error; for the J = 2 spectrum, these g-factors are much more accurate [19] than those obtained from the X-band EPR data [8]. The averaged g_J values for J = 2 are equal to 0.66663 and for J = 3 it is 0.33340 in the S-bands ESR components [13]. Then, the authors [13] solved a system of two equations for two J values $\frac{2}{3}g_L - \frac{1}{3}g_r = g_J$ for J = 2 and $\frac{1}{3}g_L - \frac{2}{3}g_r = g_J$ for J = 3 and found finally $g_r = -1.70 \times 10^{-4}$ ($g_L = 0.99986$). The late value for g_L of Arrington et al. [13] is in good agreement with more accurate full EPR spectrum analysis of Miller [20], but the rotational g_r-factor resolved by Miller is different, $g_r = -1.234 \pm 0.025 \times 10^{-4}$, which is outside an experimental error [13,20]. Thus, the orbital magnetic moment of the O_2 ($^1\Delta_g$) molecule is slightly different from a simple $2\mu_B$ value and this difference is crucial for the splitting between the quartet EPR lines, which appear through the second-order corrections [20]. We will remind the reader that $g_r = {g_r}^e + {g_r}^N = {g_r}^e + 2.723 \times 10^{-4}$; thus, the rotational g_r-factor represents a difference between two comparable values. Electronic contribution (${g_r}^e$-factor) being almost equal to

-3.96×10^{-4} for the O_2 ($^1\Delta_g$) state and simultaneously close to $g_r{}^e$-value for the ground dioxygen O_2 ($^3\Sigma_g{}^-$) state causes some doubts in researchers since Equation (4) provides different origins for both states [13,20]. Indeed, only $^3\Pi_g$ states of $^1O_2$ can contribute to the $g_r{}^e$-value for the ground triplet dioxygen [22,25].

The excited O_2 ($^1\Delta_g$) is usually produced in the presence of great excess of the triplet ground state oxygen [9,27]. Thus, both ESR signals appear simultaneously in the same magnetic field ranges and the triplet ground state oxygen lines are used as an internal standard for the singlet excited O_2 ($^1\Delta_g$) concentrations measurements [9,13]. However, the nature of the ESR signal for both states of dioxygen $^3\Sigma_g{}^-$, $\Lambda = 0$ and $^1\Delta_g$, $\Lambda = 2$ is rather different. The triplet state EPR transitions frequency is determined by spin g-factor ($g^{\perp} = 2.0052$) and by its anisotropy with $g^{||} = g_e$ parameter induced by SOC mixing, while the singlet delta dioxygen exhibits nearly symmetric quartet splitting due to electron-rotational interaction when O-O bond axes rotate around two perpendicular directions. In the late case, a value of rotational B_e constant determines the spitting of the quartet lines. Understanding this qualitative difference is essential for the choice of the field strength and microwave EPR frequency range for detection of both the ground $^3O_2$ ($^3\Sigma_g{}^-$) and the excited $^1O_2$ ($^1\Delta_g$) dioxygen.

Intensity analysis of the O_2 singlet–triplet transitions in the visible (λ 760 nm) and near IR (λ 1.27 μm) regions indicates that these bands have a magnetic-dipole origin and are induced by spin–orbit coupling (SOC) [21,22]. In optical spectroscopy, the ground is denoted by the letter X and excited states of other multiplicity are enumerated by small Latin letters *a*, *b*, etc. [4]. The weak intensity of the O_2 ($X^3\Sigma_g{}^-$)- O_2 ($a^1\Delta_g$) band is determined by the same SOC-induced mixing with the $^{1,3}\Pi_g$ states which are responsible for rotational $g_r{}^e$-values in the ground triplet and the singlet excited O_2 states with similar contributions of the orbital angular momentum, Equation (4) [28–30]. At the same time, the spin g-factor of the O_2 ($X^3\Sigma_g{}^-$) state also depends on the similar orbital angular momentum contributions [22]. A good agreement of all these calculations with experimental EPR and optical data support the reliability of the similar $g_r{}^e$-values for both O_2 ($X^3\Sigma_g{}^-$) and O_2 ($a^1\Delta_g$) states.

5. Nitric Oxide

Let us consider a free radical ^2NO ($^2\Pi_{1/2}$), see Scheme 1 and Table 1. It has $S = 1/2$, $S_z = \pm 1/2$, $\Lambda = 1$. The total angular momentum about the molecular axis (neglecting rotation) is defined as $J = |\Lambda + S_z|$. The lowest state of ^2NO radical has $J = 1 - \frac{1}{2} = \frac{1}{2}$. Since the open–shell is occupied less than one-half (two double degenerate molecular orbitals (MO). These two MO has only one electron, and we get the regular spin–orbit coupling splitting. A formula for the spin g-factor of a diatomic radical has a factor ($\Lambda - 2S$) which is 0 for the current state [13]. That means $^2\Pi_{1/2}$ state has g = 0 and is diamagnetic in both gas and liquid states due to a cancellation of orbital and spin angular momenta.

The next excited state of ^2NO is $^2\Pi_{3/2}$, where $S = \frac{1}{2}$, $\Lambda = 1$. This state has $J = 1 + 1/2 = 3/2$. $J = 3/2$ splits in an external magnetic field into four sublevels M_J with quantum numbers $-3/2$, $-1/2$, $+1/2$, $+3/2$. Thus, one expects three ESR transitions with the following changes in M_J: $-3/2 \rightarrow -1/2$; $-1/2 \rightarrow +1/2$; $+1/2 \rightarrow +3/2$. The first spectra of ^2NO ($^2\Pi_{3/2}$) demonstrated namely three components [2,7,10]. Non-magnetic $^2\Pi_{1/2}$ and paramagnetic $^2\Pi_{3/2}$ states of ^2NO are very close in their energies. The excited state $^2\Pi_{3/2}$ is only 1.43 kJ/mole higher in energy than the ground $^2\Pi_{1/2}$ state [14]. Let us consider the factors, which determine this energy splitting. The open-shell wave function of the doublet $^2\Pi_J$ state can be presented in the following forms: for the case of less-than-half occupied open π–shell we use Equation (5). We use Equation (6) for the case of more-than-half occupied π–shell [31]:

$$^2\Pi_J = \frac{1}{\sqrt{2}}(\pi_x \pm i\pi_y)^2\Pi_J = \frac{1}{\sqrt{2}}(\overline{\pi}_x \mp i\overline{\pi}_y) \quad (5)$$

$$^2\Pi_J = \frac{1}{\sqrt{2}}(|\pi_y\overline{\pi}_y\pi_x| \pm i|\pi_x\overline{\pi}_x\pi_y|)^2\Pi_J = \frac{1}{\sqrt{2}}(|\pi_y\overline{\pi}_y\overline{\pi}_x| \mp i|\pi_x\overline{\pi}_x\overline{\pi}_y|) \quad (6)$$

The Left and right parts of Equations (5) and (6) are the equivalent ways to present the electronic configuration of the same state. π and π with a bar on the top are used to distinguish the spin state of a spin orbital. One spin orbital may have s = $\frac{1}{2}$ and the other will have s = $-1/2$ and vice versa.

The upper sign in these equations corresponds to $J = 3/2$ and the lower sign corresponds to $J = 1/2$. The imaginary form of wave function is necessary to satisfy the requirement $L_z\Psi = \Lambda h\Psi$. We use here a common notation for the Slater determinant of many-electron wave function [5]. Spin–orbit coupling (SOC) operator can be used in a simple effective single-electron form [31,32]:

$$H_{SOC} = \sum_i \sum_A \zeta_{n,l}^A \vec{l}_{i,A} \vec{s}_i = \sum_i \vec{B}_i \vec{s}_i \tag{7}$$

where $\zeta_{n,l}^A$ is the SOC constant for the valence shell of atom A, $\vec{l}_i$ and $\vec{s}_i$ are orbital and spin angular momentum operators, respectively for the i-th electron. The SOC constants obtained from atomic spectra are equal $\zeta_{2p}^N = 73$ cm^{-1} and $\zeta_{2p}^O = 153$ cm^{-1} for nitrogen and oxygen, respectively [31]. Since $J = |\Lambda + S_z|$, there are two possible presentations for each J. Expectation energy of the SOC operator is equal

$$\varepsilon_J = \left\langle {}^2\Pi_J | H_{SOC} | {}^2\Pi_J \right\rangle = \pm\frac{i}{4}[\langle \pi_x | B_z | \pi_y \rangle - \langle \pi_y | B_z | \pi_x \rangle] \tag{8}$$

Let us take $2\pi^*$-molecular orbital of ^{2}NO radical from the SCF calculation with the zero differential overlap approach within PM-3 method [33]: $2\pi_{x(y)} = 0.811\psi_{p_{x(y)}}^N - 0.585\psi_{p_{x(y)}}^O$. This form of 2π-MO is in good agreement with the hyperfine coupling parameters fitting to ESR spectrum of gaseous ^{2}NO molecule [34]. Using these MO LCAO ($C_{p_{x(y)}}^A$) coefficients we obtain the following splitting:

$$\varepsilon_{3/2} - \varepsilon_{1/2} = \sum_A (C_{p_{x(y)}}^A)^2 \zeta_{2p}^A = 100.4 \text{ cm}^{-1} = 1.2 \text{ kJ/mol}, \tag{9}$$

which is in reasonable agreement with the experiment [23]. Even such a simple semi-empirical approach provides a quantitative explanation of the fine structure SOC splitting in ^{2}NO radical.

$^2\Pi_{3/2}$ is easily accessible at room and lower temperatures; the thermal energy at room temperature is 2.5 kJ/mol. Thus, one can observe the X-band ESR spectrum of the excited $^2\Pi_{3/2}$ state, which is presented in Figure 3:

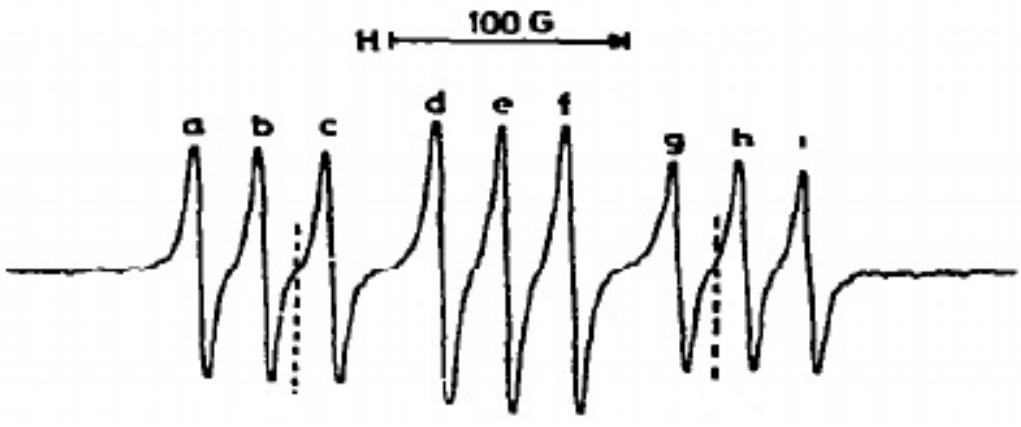

Figure 3. ESR spectrum of ^{2}NO ($^2\Pi_{3/2}$) at room temperature and pressure P_{NO} = 0.5 Torr. Vertical dashed lines mark the central part of the spectrum. Adapted from ref. [10].

One can see that each of the three major components splits into three components due to hyperfine coupling (HFC) with ^{14}N nucleus. A highly resolved spectrum of ^{2}NO ($^{2}\Pi_{3/2}$) has 27 components due to additional interactions [10]. We calculated the HFC tensor for ^{14}N isotope of ^{2}NO radical by density functional theory with B3LYP/6–311++G(dp) approach [33]; the isotropic HFC constant a = 11.386 MHz, anisotropic HFC tensor component along the z-axis is equal 74.673 MHz. The oxygen atom bears an electric charge of +0.091 e and spin density of 0.286, whereas the nitrogen has −0.091 e and 0.714, respectively. Other spectroscopic parameters are in a good agreement with experiment [23]: r_e = 1.148 Å, ν_e = 1980 cm^{-1}, B_e = 51.364 GHz, averaged polarizability α_{av} = 9.4 a_0^3, dipole moment is equal −0.13 debye. The relatively small polarity and polarizability of ^{2}NO radical explain its rather weak intermolecular interaction in the gas phase; thus its ESR spectrum at moderate pressure does not depend on the properties of foreign gases. The calculated HFC tensor of ^{2}NO radical with natural isotope abundance does not contradict to experimental ESR spectrum (Figure 3) [10].

The first EPR spectrum of nitric oxide, ^{2}NO ($^{2}\Pi_{3/2}$) was tentatively interpreted as being due to traditional magnetic–dipole transitions (MDT), since the MDT nature is typical for EPR signals [10]. However, the latter the electric–dipole transitions (EDT) were shown to be more intense and prominent in this EPR spectrum. As many other $^{2}\Pi$ states the ^{2}NO ($^{2}\Pi_{3/2}$) state demonstrates a clear Λ–doubling effect [14]. The EDT lines occur between opposite members of an Λ-doublet (- ↔ +), while much weaker MDT transitions connect the same Λ-doublet members (- ↔ -) or (+ ↔ +) [4]. All these features are determined by relatively strong SOC (Equation (8)) in quasi degenerate $2\pi_x$- and $2\pi_y$- molecular orbitals of nitric oxide.

It is interesting to note that in homonuclear dioxygen molecules, all EDT's are strongly forbidden by the central point (inversion) symmetry and only weak MDT are observed in the low-pressure gas phase in the triplet–singlet *b*-*X* and *a*-*X* transitions in the visible and near IR regions [21]. However, the release of symmetry restriction in solvents permits the O_2 ($X^3\Sigma_g^-$)- O_2 ($a^1\Delta_g$) band at 1.2 μm to acquires EDT character and become much more intense because of strong spin–orbit coupling inside the dioxygen O_2 (π_g) open shell. Thus, many peculiarities of the optical and EPR spectra of two diatomic species, ^{2}NO and O_2, being very important for atmospheric problems, strongly depend on spin–orbit coupling in $2\pi^*$- orbitals (Scheme 1) which energy does not exceed 1–2 kJ/mol [21,32].

Spin and rotational energies depend upon each other. Collisions of ^{2}NO ($^{2}\Pi_{3/2}$) with solvent molecules lead to a spin relaxation or an infinite boarding of components. Note, that gas-phase ESR spectra are observed at low pressure. An increase in pressure leads to the broadening of components.

6. ESR of Trapped ^{2}NO

^{2}NO is used as a probe of surfaces, different cages, nano-objects, and biological species. Adsorption of ^{2}NO on surface vacancies, inside zeolites [11,15], or the C_{60} cavity [16], complexation with biological molecules [18] leads to a quenching of the orbital momentumΛ; thus, the lowest $^{2}\Pi_{1/2}$ state of ^{2}NO becomes paramagnetic and demonstrates ESR. In the adsorbed ^{2}NO species, the $2\pi_x$- and $2\pi_y$- molecular orbitals (MO) are split by interaction with the surface and the energy splitting between the perturbed $2\pi_x$ and $2\pi_y$ MO is a measure of the spin g-factor anisotropy [11]. ^{2}NO species is not any more an object of diatomic spectroscopy with proper quantization of orbital and rotational angular momenta. Instead, the polyatomic cluster is an object of the ground and excited states studies. The principal values of the g-tensor are used now to determine the MO splitting to characterize the electric field strength at the ^{2}NO adsorption site. An example is presented in Figure 4:

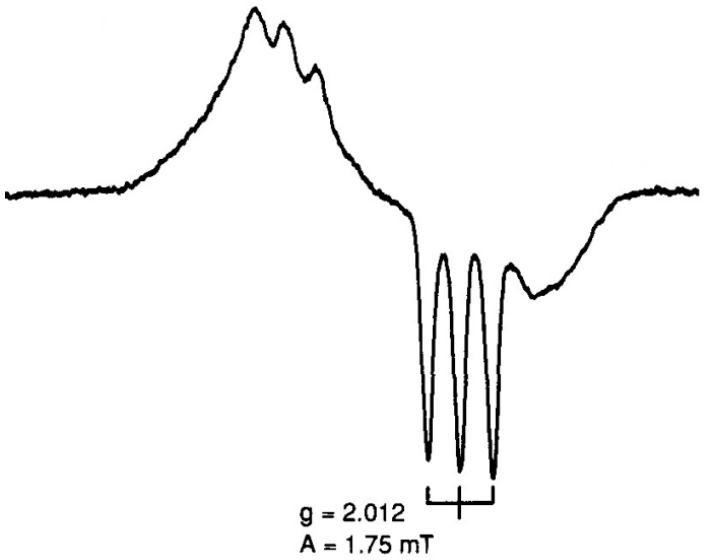

Figure 4. ESR spectrum of an adduct of ^{2}NO and hemoglobin at 90 K. Adapted from ref. [18]; see for details ref. [18].

The sharp downward components (Figure 4) arise due to hyperfine coupling on ^{14}N nucleus of a bound ^{2}NO and the g-factor just shows the position of the ESR signal.

To obtain an interpretation of the ESR spectrum in Figure 4, we simulated the ^{2}NO complex with hemoglobin model by quantum chemical DFT calculation (Figure 5) in the framework of B3LYP/6–31 G approach [33]. The Fe-N coordination bond length is optimized to be 0.1866 nm with the angle Fe-N-O = 121.4°, the distance Fe-Cl = 0.2186 nm just simulates the Fe ion coordination with the protein residue. The calculated g-factor has components 2.0137, 20,082, and 1.9843, which are in qualitative agreement with the ESR spectrum in Figure 4. A large portion of nonpaired spin is concentrated on Fe ions.

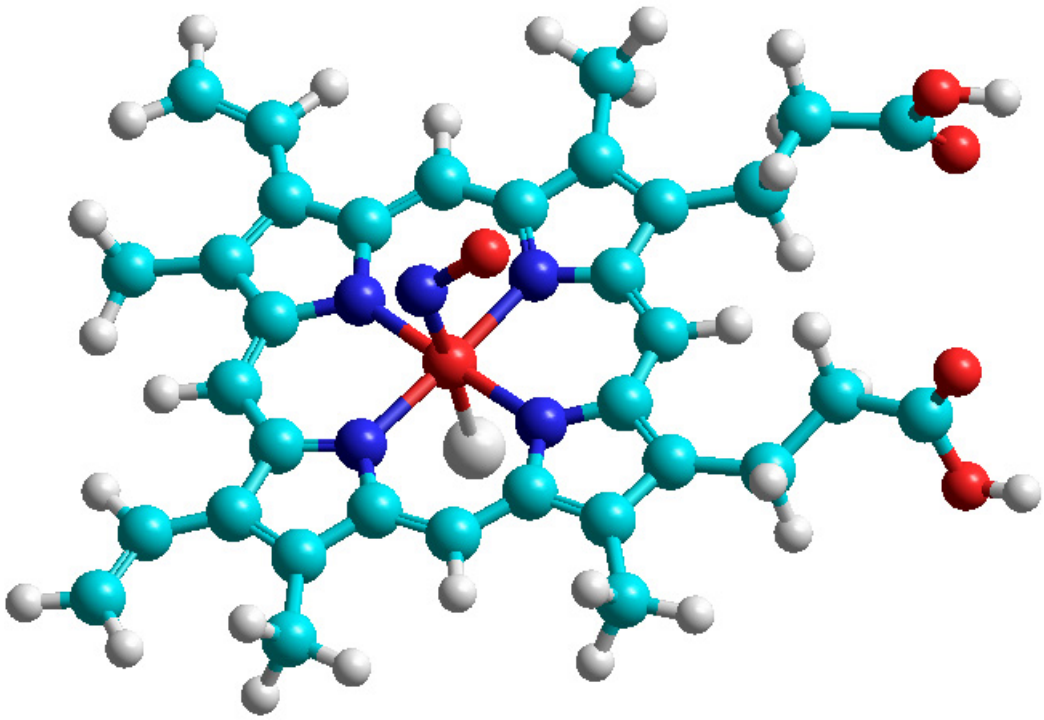

Figure 5. The model of the ^{2}NO adduct with hemoglobin (coordinated with Cl^{-} anion as a model of protein residue). Red color for O and Fe atoms, dark blue N, blue C, and grey for H atoms. Adapted from ref. [29]. This is also a calculation made for this paper.

The calculated isotropic HFC constant on the ^{14}N nucleus is equal to a = 15.78 MHz; anisotropic HFC tensor components are calculated at −30.2, −7.3, and 37.5 MHz. Thus, the Fermi-coupling a constant is slightly increased by 4.4 MHz in comparison with free NO radical, but the components of the HFC tensor are approximately half-diminished upon ^2NO coordination to the iron center of hemoglobin. The Fe(II) ion provides a rather strong influence on the hyperfine structure of the EPR spectrum of nitric oxide.

These results are comparable with our previous theoretical DFT studies of ^2NO and O_2 interactions with hemoglobin [28,29]. Hyperfine coupling on^{14}N nucleus is in agreement with the theory of the nitric oxide ESR spectrum made as early as 1950 [30].

7. Conclusions and Perspectives

A newcomer may be very surprised that a *singlet* molecule $^1O_2$ demonstrates an ESR spectrum in the gas phase. Due to the lack of spin in the molecule, it is better to use the term Electron Paramagnetic Resonance, which is achieved in this case where paramagnetism is due to the orbital momentum. The *radical* ^2NO does not demonstrate the ESR spectrum in liquid solutions. ESR of these and other states can be understood considering the terms of these diatomic molecules.

^2NO is an atmospheric pollutant. ^2NO reacts with dioxygen and produces $^2NO_2$, which is a pollutant as well. In the literature on environmental problems, both pollutants are often called NOx.

Air pollutant singlet dioxygen has a relatively short lifetime from milliseconds to less than 10 s [14]. Specific lifetime depends upon pressure and the presence of quenchers of $^1O_2$. In the air atmosphere (P_{tot} = 1 atm), $^1O_2$ has a lifetime of 2.8 s measured with a quencher [19]. During this time, $^1O_2$ diffuses approximately 1 cm [19].

The gas pollutants exist in most cases in the presence of dioxygen. One or another strong line of ESR of $^3O_2$ ($^3\Sigma_g^-$) (Figure 1) can serve as a convenient internal standard for monitoring $^1O_2$ ($^1\Delta_g$) or other gas pollutants.

Author Contributions: Conceptualization: I.V.K. and B.F.M., Methodology: B.F.M. and I.V.K., Software: B.F.M., Formal anlysis: B.F.M. and I.V.K., Original draft preparation: B.F.M. and I.V.K. Both authors have read and agreed to the published version of the manuscript.

Funding: This research received no additional funding.

Institutional Review Board Statement: Institutional Review Board Statement BK 567, 05/12/2021.

Informed Consent Statement: Informed consent was obtained from all subjects involed in the study.

Data Availability Statement: The data presented in this study are available on request from the corresponding author. 05/13/2021.

Conflicts of Interest: There is no conflict of interest.

References

1. Arnhold, J. *Cell and Tissue Destruction: Mechanisms, Protection, Disorders*; Academic Press: London, UK, 2020.
2. Weil, J.A.; Bolton, J.R.; Wertz, J.E. *Electron Paramagnetic Resonance. Elementary Theory and Practical Applications*; Wiley: New York, NY, USA, 1994.
3. Tinkham, M.; Strandberg, M.W.P. Theory of the fine structure of the molecular oxygen ground state. *Phys. Rev.* **1955**, *97*, 937–1024. [CrossRef]
4. Herzberg, G. *Molecular Spectra and Molecular Structure. I. Spectra of Diatomic Molecules*; Van Nostrand: New York, NY, USA, 1950.
5. Murrell, J.N.; Kettle, S.F.A.; Tedder, J.M. *Valence Theory*; Wiley: London, UK, 1965.
6. Khudyakov, I.V.; Serebrennikov, Y.A.; Turro, N.J. Spin-orbit coupling in free-radical reactions: On the way to heavy elements. *Chem. Rev.* **1993**, *93*, 537–570. [CrossRef]
7. Kon, H. Parmagnetic resonance of molecular oxygen in condensed phases. *J. Am. Chem. Soc.* **1973**, *95*, 1045–1049. [CrossRef]
8. Carrington, A. *Microwave Spectroscopy of Free Radicals*; Academic Press: London, UK, 1974.
9. Ruzzi, M.; Sartori, E.; Moscatelli, A.; Khudyakov, I.V.; Turro, N.J. Time-resolved EPR study of singlet oxygen in the gas phase. *J. Phys. Chem. A* **2013**, *117*, 5232–5240. [CrossRef] [PubMed]
10. Jinguji, M.; Ohokubo, Y.; Tanaka, I. High resolution EPR spectrum of nitric oxide in the gas phase. *Chem. Phys. Lett.* **1978**, *54*, 136–138. [CrossRef]

11. Pöppl, A.; Rudolf, T.; Manikandan, P.; Goldfarb, D. W- and X-Band Pulsed Electron Nuclear Double-Resonance Study of a Sodium−Nitric Oxide Adsorption Complex in NaA Zeolites. *J. Am. Chem. Soc.* **2000**, *122*, 10194–10200. [CrossRef]
12. Falick, A.M.; Mahan, B.H.; Myers, R.J. Paramagnetic resonance spectrum of 1Δg oxygen molecule. *J. Chem. Phys.* **1965**, *42*, 1837–1840. [CrossRef]
13. Arrington, C.A.; Falick, A.M.; Myers, R.J. Electron paramagnetic resonance spectrum of O2(1Δg)—Its 17O hyperfine coupling and electronic and rotational g values. *J. Chem. Phys.* **1971**, *55*, 909–917. [CrossRef]
14. Hasegawa, K.; Yamada, K.; Sasase, R.; Miyazaki, R.; Kikuchi, A.; Yagi, M. Direct measurements of absolute concentration and lifetime of singlet oxygen in the gas phase by electron paramagnetic resonance. *Chem. Phys. Lett.* **2008**, *457*, 312–314. [CrossRef]
15. Lunsford, J.H. Surface interactions of NaY and decationated Y zeolites with nitric oxide as determined by electron paramagnetic resonance spectroscopy. *J. Phys. Chem.* **1968**, *72*, 4163–4168. [CrossRef]
16. Dinse, K.-P.; Kato, T.; Hasegawa, S.; Hashikawa, Y.; Murata, Y.; Bittl, R. EPR study of NO radicals encased in modified open C 60 fullerenes. *Magn. Reson.* **2020**, *1*, 197–207. [CrossRef]
17. Scalabrin, A.; Saykally, R.J.; Evenson, K.M.; Radford, H.E.; Mizushima, M. Laser magnetic resonance measurement of rotational transitions in the metastable a1Δg state of oxygen. *J. Mol. Spectrosc.* **1981**, *89*, 344–351. [CrossRef]
18. Westenberer, U.; Thanner, S.; Ruf, H.H.; Gersonde, K.; Sutter, G.; Trentz, O. Formation of free radicals and nitric oxide derivative of hemoglobin in rats during shock syndrome. *Free Rad. Res. Commun.* **1990**, *11*, 167–178. [CrossRef]
19. Vahtras, O.; Minaev, B.; Ågren, H. Ab initio calculations of electronic g-factors by means of multiconfiguration response theory. *Chem. Phys. Lett.* **1997**, *281*, 186–192. [CrossRef]
20. Huber, K.P.; Herzberg, G. *Molecular Spectra and Molecular Structure. IV. Constants of Diatomic Molecules*; Van Nostrand Reinold: New York, NY, USA, 1979.
21. Minaev, B.F. Electronic mechanisms of molecular oxygen activation. *Russ. Chem. Rev.* **2007**, *76*, 989–1011. [CrossRef]
22. Wang, K.-K.; Song, S.; Jung, S.-J.; Hwang, J.-W.; Kim, M.-G.; Kim, J.-H.; Sung, J.; Lee, J.-K.; Kim, Y.-R. Lifetime and diffusion distance of singlet oxygen in air under everyday atmospheric conditions. *Phys. Chem. Chem. Phys.* **2020**, *22*, 21664–21671. [CrossRef]
23. Miller, T.A. Rotational Moment, Rotational g Factor, Electronic Orbital g Factor, and Anisotropy of the Magnetic Susceptibility of 1 Δ O_2. *J. Chem. Phys.* **1971**, *54*, 330–337. [CrossRef]
24. Sauer, S.P.A. Communication: Rotational g-factor and spin-rotation constant of CH^+. *J. Chem. Phys.* **2010**, *133*, 171101. [CrossRef]
25. Engström, M.; Minaev, B.; Vahtras, O.; Ågren, H. Linear response calculations of electronic g-factors and spin-rotational coupling constants for diatomic molecules with a triplet ground state. *Chem. Phys.* **1998**, *237*, 149–158. [CrossRef]
26. Minaev, B.F. Effect of spin-orbit coupling on the intensity of magnetic dipole transitions in molecular oxygen. *Soviet Phys. J.* **1978**, *21*, 1205–1209. [CrossRef]
27. Frisch, M.J.; Trucks, G.W.; Schlegel, H.B.; Scuseria, G.E.; Robb, M.A.; Cheeseman, J.R.; Scalmani, G.; Barone, V.; Petersson, G.A.; Nakatsuji, H.; et al. *Gaussian 09, 2009, Revision C.02*; Gaussian: Wallingford, CT, USA, 2009.
28. Zakharov, I.I.; Minaev, B.F. DFT calculations of the intermediate and transition state in the oxidation of NO by oxygen in the gas phase. *Theor. Exp. Chem.* **2011**, *47*, 93–100. [CrossRef]
29. Minaev, B.F.; Minaeva, V.A. Spin-dependent binding of dioxygen to heme and charge-transfer mechanism of spin-orbit coupling enhancement. *Ukr. Bioorg. Acta* **2008**, *2*, 56–59.
30. Minaev, B.F. Theory of the solvent effect on the radiative probability of the a1Δg-X3Σg transition in the oxygen molecule. *Opt. Spectrosc.* **1985**, *58*, 761–763.
31. Minaev, B.F. Spin alignment of the triplet state and new methoids of the phosphoiresce study. *Phys. Mol.* **1979**, *7*, 34–40. (In Russian)
32. Dousmanis, G.C. Magnetic hyperfine effects and electronic structure of NO. *Phys. Rev.* **1955**, *97*, 967. [CrossRef]
33. Minaev, B.F.; Zahradnik, R. Calculations of quartet state spectra for diatomic species by INDO CI method including spin-orbit coupling perturbation. *Collec. Czehoslovak Chem. Commun.* **1981**, *46*, 179–193. [CrossRef]
34. Bregnhøj, M.; Westberg, M.; Minaev, B.F.; Ogilby, P.R. Singlet oxygen photophysics in liquid solvents: Converging on a unified picture. Accounts of chemical research. *Acc. Chem. Res.* **2017**, *50*, 1920–1927. [CrossRef] [PubMed]